scientific reports

Check for updates

OPEN

Green production of silver nanoparticles from *Cassia occidentalis* and *Alternanthera pungens* and evaluation of their nematicidal activity against *Meloidogyne javanica*

Navaneetha Krishnan Ayyankalai[1], Palanisamy Sundararaj[1], Manikantan Gurumoorthy Baskar[2], Nallusamy Duraisamy[3]✉, Sakthivel Muthu[4]✉, Mythileeswari Lakshmikanthan[5] & Gholamreza Abdi[6]✉

In this study, silver nanoparticles (AgNPs) were synthesized through an eco-friendly bioreduction process using plant extracts from *Cassia occidentalis* and *Alternanthera pungens*. The formation of AgNPs was confirmed by a visible color change in the reaction mixture, followed by characterization using UV-Vis spectroscopy, SEM-EDX, FTIR, XRD, zeta potential, and dynamic light scattering (DLS) analysis. UV-Vis spectroscopy revealed characteristic surface plasmon resonance (SPR) peaks at 420 nm and 425 nm for *C. occidentalis* and *A. pungens*, respectively. EDX analysis confirmed a high silver content, while SEM images depicted irregularly distributed nanoparticles with spherical and cylindrical morphologies. FTIR spectra indicated the involvement of various functional groups in nanoparticle stabilization, and XRD analysis verified their crystalline structure. DLS measurements indicated an average nanoparticle size of approximately 100 nm, while zeta potential analysis suggested good colloidal stability. The nematicidal potential of AgNPs was assessed against second-stage juveniles (J2) of *Meloidogyne incognita*, exhibiting dose-dependent toxicity with an LC_{50} value of 0.5 mg/L. Field experiments on tomato plants demonstrated a significant reduction in nematode infestation at higher AgNP concentrations, highlighting their potential as an eco-friendly alternative for nematode management in agriculture.

Keywords Silver nanoparticles (AgNPs), Bioreduction, Characterization, Nematicidal activity, Meloidogyne incognita

Nematology, a vital branch of biological sciences, focuses on nematodes, a diverse group of roundworms prevalent across various environments worldwide. Commonly referred to as "eelworms" in Europe, "nemas" in the United States, and roundworms by zoologists, nematodes represent the most numerous multicellular metazoans on Earth. These unsegmented, pseudocoelomate worms inhabit both marine and terrestrial ecosystems and include free-living, plant-parasitic, animal-parasitic, and entomopathogenic species[1,2].

Historically, the scientist Borellus first documented a free-living nematode, "vinegar eel" (*Turbatrix aceti*)[3] while scientist Needham identified the first plant-parasitic nematode (*Anguina tritici*) in wheat seeds[4,5]. Root-knot nematodes, particularly *Meloidogyne* species, discovered by Berkeley[6] are notorious for their global

[1]Department of Zoology, Bharathiar University, Coimbatore, Tamil Nadu 641 046, India. [2]Department of Zoology, The American College, Madurai, Tamil Nadu 625 002, India. [3]Department of Research, Meenakshi Academy of Higher Education and Research (MAHER), Chennai, Tamil Nadu 600 078, India. [4]Department of Dermatology, Saveetha Medical College and Hospital, Saveetha Institute of Medical and Technical Sciences (SIMATS), Thandalam, Chennai, Tamil Nadu 602105, India. [5]Department of Biotechnology, University of Madras, Guindy Campus, Chennai, Tamil Nadu 600025, India. [6]Department of Biotechnology, Persian Gulf Research Institute, Persian Gulf University, Bushehr, Iran. ✉email: nallfree07@gmail.com; saktthivel@gmail.com; abdi@pgu.ac.ir

distribution and significant agricultural impact[4,7]. These obligate plant parasites induce gall formation on roots, leading to substantial crop losses estimated at $78 billion globally and $8 billion in the U.S. alone[8,9]. In India, root-knot nematodes were first reported affecting tea plantations in Kerala[7,10]. Nanotechnology offers promising solutions for nematode management. Nanoparticles (NPs), which have a size range of 1 to 100 nm and are used in biotechnology, environmental sciences, and pharmaceuticals, have unique qualities because of their large surface area and small size[11–13].

Biosynthesis of nanoparticles from plant materials is an economical and environmentally responsible substitute for traditional techniques. It avoids hazardous chemicals and harsh environments[14,15]. Actinobacteria, fungi, algae, and plants are among the biological systems that have been investigated for the synthesis of nanoparticles[16–18].

Silver nanoparticles (AgNPs) are notable by their antimicrobial capabilities, demonstrating antibacterial, antifungal, antiviral and larvicidal actions[19–21]. This study assessed the nematicidal efficacy of silver nanoparticles derived from the medicinal plants *Cassia occidentalis* and *Alternanthera pungens* against the plant–parasitic nematode *Meloidogyne incognita*. Belong to the leguminous family, is conventionally employed to address diverse diseases, such as inflammation and hepatic disorder[22–24]. *Alternanthere pungens*, a member of the Amarnathaceae family, is recognized for its diuretic characteristic and medicinal uses in the treatment of jaundice and gonorrhoea[25,26].

In the present investigation, the plant–parasitic nematode Meloidogyne incognita was used to test the nematicidal potential of silver nanoparticles made from the medicinal plants Alternanthera pungent *and Cassia occidentalis*.

Experimental and methods

Collection and Preparation of plant materials

In the southern districts of Sivganga, Ramanathapuram, Tamil Nadu, India, samples of *Alternanthera pungens* and *Cassia occidentalis* were collected. The authenticated samples are held by the Department of Zoology at Bharathiar University in Coimbatore, India. The collected specimens were subsequently identified and authenticated by the Botanical Survey of India (BSI). The assigned specimen numbers were BSI/SRC/5/23/10–11/Tech.145,908 for *Alternanthera pungens* and BSI/SRC/5/23/10–11/Tech.423 for *Cassia occidentalis*. The leaves of both plants were thoroughly rinsed with running tap water to remove any debris and then dried in the shade for ten days. Once dried, the leaves were ground into a fine powder using a mechanical grinder. The resulting powder was sieved through a 22-mesh sieve to ensure uniform particle size (Fig. 1).

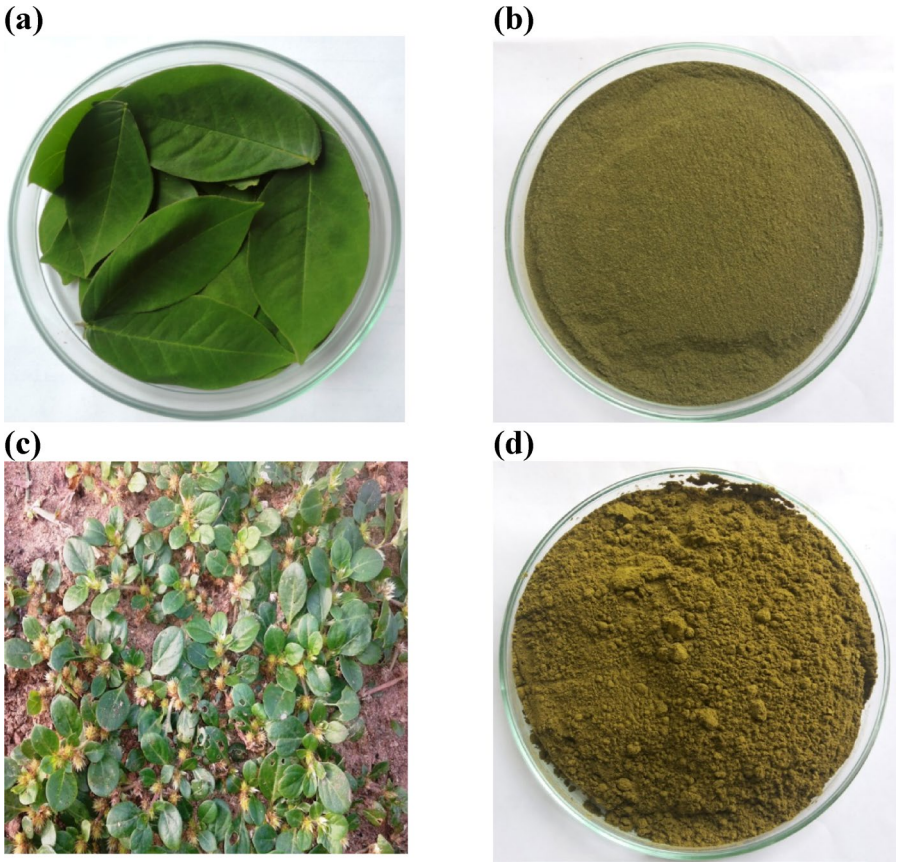

Fig. 1. The collected plants, *C. occidentalis* and *A. pungens*, are shown in images **(a)** and **(c)**, respectively. After collection, the plants were shade-dried and ground into a fine powder, as depicted in images **(b)** and **(d)**.

Extraction of plant compounds

For the preparation of aqueous extracts, 5 g of the powdered plant material was boiled in 100 mL of distilled water. After boiling, the mixture was allowed to cool to room temperature, then filtered using Whatman No. 1 filter paper. The filtrates were stored at 4 °C until further use. These plant extracts acted as reducing agents for the synthesis of silver nanoparticles by reacting with 0.1 M silver nitrate ($AgNO_3$).

Collection of tomato roots and extraction of M. incognita eggs

Roots from *M. incognita* infected tomato plants were harvested from agricultural fields located in Thondamuthur, Coimbatore district, India. The tomato plants infected with *Meloidogyne incognita* were collected from agricultural fields with the full knowledge and permission of the landowner. A formal consent for sample collection was obtained prior to the study. The collected roots were carefully rinsed under running tap water to eliminate any attached soil particles and other contaminants. Root galls were examined, which housed adult females containing egg masses at their posterior ends. These eggs were embedded within a gelatinous matrix. Each female nematode was observed to produce approximately 400 to 500 eggs. Tomato roots were finely chopped and immersed in a 1% sodium hypochlorite (NaOCl) solution to dissolve the gelatinous matrix surrounding the nematode eggs. The mixture was agitated vigorously for 5 min to ensure effective digestion. Following this, the root fragments were thoroughly rinsed with distilled water to eliminate any residual sodium hypochlorite. The washed root material was then sequentially passed through a series of sieves with mesh sizes of 72, 100, 200, and 500. The *M. incognita* eggs were subsequently collected from the residue retained on the 500-mesh sieve (0.05 µm). Eggs were incubated and allowed to hatch using a modified Baermann funnel technique. This method involved placing a concave steel mesh covered with Whatman No. 1 filter paper in a Petri dish containing water. The first molt occurred within the eggs, leading to the emergence of second-stage juveniles. These juveniles passed through the filter paper and settled at the bottom of the Petri dish for collection.

Biosynthesis of silver nanoparticles

Silver nanoparticles (AgNPs) were synthesized using plant extracts from *C. occidentalis* and *A. pungens*. In this process, 20 mL of each plant extract was separately mixed with 100 mL of 0.01 M silver nitrate ($AgNO_3$) solution, prepared by dissolving 0.169 g of $AgNO_3$ in distilled water, maintaining a 1:4 ratio of extract to silver nitrate solution, the mixtures were stirred at 360 rpm using a magnetic stirrer for 4 h. A gradual color change from pale yellow to dark brown was observed, indicating the reduction of silver ions and the formation of AgNPs. The formation of silver nanoparticles was confirmed through UV-Vis spectrophotometric analysis within the wavelength range of 350 nm to 550 nm. The colloidal silver nanoparticle solutions were centrifuged at 5000 rpm for 30 min to filter the nanoparticles. This procedure was carried out three times to ensure that all remaining contaminants were eliminated. To prevent the nanoparticles from aggregating, the resultant pellets were collected and sonicated for three hours. Through UV-vis spectrophotometric methods, the presence of AgNPs nanoparticles within the wavelength range of 350–550 nm was confirmed. The colloidal solutions were centrifuged at 5000 rpm for thirty minutes to filter the nanoparticles. This method was performed three times to ensure the removal of any residual impurities. To prevent the nanoparticles from aggregating, the resultant pellets were collected and sonicated for 3 h. After sonication, the samples were placed on a glass plate and allowed to dry for twelve hours at 60 °C in a hot air oven. As the final form of silver nanoparticles, the dried powdered material was collected and stored for further use analysis.

Characterization of silver nanoparticles

UV–Visible spectral analysis

The synthesized silver nanoparticle (AgNP) using extracts of *C. occidentalis* and *A. pungens* was determined using UV-visible spectroscopy. The formation and bio-reduction of AgNPs reaction aliquots collected at regular intervals and allowed for the confirmation of AgNP. UV-visible spectroscopy was used to examine these samples absorbance that would suggest the formation of nanoparticles. The Vasco 1301 spectrophotometer, which was used in the wavelength range of 200–800 nm with a resolution of 1 nm, the absorption spectra of the reaction mixtures were captured. Through the measurement of absorbance at different time periods, the reaction was confirmation of indicating the effective synthesis of AgNPs.

Scanning Electron microscopic (SEM) analysis with energy dispersive x-ray

The surface morphology of AgNPs nanoparticles was investigated using a scanning electron microscope (Quanta FEG 250, FEI Company). The colloidal silver nanoparticle solution was centrifuged for 30 min at 5000 rpm to prepare the sample. The pellet was redispersed in distilled water and subjected to additional centrifugation three times to eliminate any residual impurities. To ensure even dispersion, the nanoparticles were sonicated for an hour after purification. The powdered nanoparticles, following sonication and suspension, were subsequently dried for 12 h at 60 °C in a hot air oven. The surface morphology of the silver nanoparticles was evaluated using SEM analysis on these powdered samples.

Energy Dispersive X-ray (EDX) analysis, usually referred to as EDS or EDAX, this technique to determine the elemental composition of a sample or a designated region within it. Coupled with a Scanning Electron Microscope (SEM), EDX identifies distinctive x-rays released during the interaction of an electron beam with the material. An EDS detector segregates x-rays into an energy spectrum, which is subsequently analyzed by specialist software to determine the existence and concentration of elements. This technique facilitates accurate chemical analysis at micron- level and may produce elemental maps across extensive regions, providing critical compositional information for diverse materials.

Fourier transform infrared (FTIR) spectroscopic analysis
Silver nanoparticles were obtained by reacting 1 mM $AgNO_3$ with leaf extracts of *C. occidentalis* and *A. pungens* for 5 h, followed by centrifugation at 10,000 rpm for 15 min at room temperature. The resultant pellet was purified and re-dispersed in sterile distilled water, and subjected to centrifugation, a procedure that was repeated three times to eliminate residual impurities. The purified AgNPs were dried and subsequently examined via FTIR spectroscopy (IR Affinity-1, Shimadzu, Tokyo, Japan) employing the KBr pellet technique in diffuse reflection mode at a resolution of 4 cm^{-1}, scanning the range of 500–4000 cm^{-1}. The same approach was employed on the leaf extracts prior to and after bioreduction for comparative analysis.

X-ray diffraction analysis
The AgNPs sample was analyzed by X-ray diffraction (XRD) with a Shimadzu XRD-6000/6100 system operating at 30 kV and 30 mA. X-ray diffraction was employed to determine the size and crystalline nature of the silver nanoparticles using Cu Kα radiation at a 2θ angle. XRD analysis is a rapid technique for determining unit cell characteristics and identifying crystalline phases. The average composition of finely ground samples was analyzed, and the Debye-Scherrer equation was utilized to ascertain particle size.

$$D = 0.94\lambda/B\cos\theta$$

Dynamic light scattering (DLS) and zeta potential analysis
The characterization of the synthesized nanoparticles involved measuring the particle size distribution through dynamic light scattering (DLS) and evaluating the surface charge via zeta potential measurements. The nanoparticle suspensions underwent centrifugation at 5000 rpm for 30 min to remove any remaining impurities. The centrifugation process was performed three times to ensure thorough purification. The AgNPs pellet was subsequently subjected to sonication for one hour to achieve uniform dispersion. The nanoparticle suspension was then diluted with distilled water to attain the appropriate concentration for analysis. The hydrodynamic diameter and zeta potential were determined using a Malvern Zetasizer Nano system (Malvern Instruments, UK).

Preparation of silver nanoparticle (AgNPs) stock solution
The stock solutions were prepared using silver nanoparticles (AgNPs) derived from *C. occidentalis* and *A. conyzoides*. A precise 100 mg of AgNPs was weighed and dissolved in 100 mL of distilled water. To minimise particle agglomeration and ensure uniform dispersion, the mixtures were sonicated for 12 h. Various concentrations required for further experimental investigation were then prepared from these stock solutions for additional analysis.

Toxicological assessment of silver nanoparticles on M. incognita
To assess the toxicological impact of silver nanoparticles (AgNPs) on second-stage juveniles (J2) of M. incognita, nematodes were subjected to various doses of AgNPs derived from *C. occidentalis* and *A. pungens*. The tested concentrations included 0.1 mg/L, 0.3 mg/L, 0.5 mg/L, 0.7 mg/L, and 1 mg/L. For each concentration, 10 mL of deionized water containing 100 nematodes (equivalent to 10 nematodes/mL) was prepared. Each concentration was tested in quintuplicate (five replicates) to ensure statistical reliability. Control groups, containing nematodes in nanoparticle-free water, were simultaneously maintained under identical conditions. Nematode mortality was recorded at 24-hour, 48-hour, and 72-hour intervals post-exposure to both types of silver nanoparticles. The mortality rate was calculated by counting the number of immobile or dead nematodes under a microscope, distinguishing them from alive, active individuals.

Infectivity assay of M. incognita treated with AgNPs
Tomato plants were cultivated in nursery trays filled with sterilized soil composed of red soil, farmyard manure, and sand mixed in a 2:1:1 ratio. After ten days of growth, *M. incognita* juveniles treated with silver nanoparticles (AgNPs) were inoculated into the tomato plants. The AgNPs used in this study were synthesized using *C. occidentalis* and *A. pungens* extracts. For each concentration tested, five replicates were maintained alongside a control group for comparison.

Root tissue staining
After one week of inoculation with second-stage juveniles (J2) of *M. incognita*, the infected plants were carefully uprooted from the nursery trays. The roots were gently detached from the plants and prepared for staining. To create the staining solution, 10 mL of lactic acid, 10 mL of phenol, and 0.001 mg of acid fuchsin were thoroughly combined. The excised roots were then immersed in 3 mL of the prepared acid fuchsin solution and briefly boiled to facilitate staining. Following boiling, the stained roots were stored for 24 h at room temperature. To remove excess stain, the roots were de-stained using phenol crystals until the background tissues appeared clear. Finally, the cleared roots were examined under a stereomicroscope to identify and count the second-stage juveniles of *M. incognita*. The number of juveniles present in the root tissues was recorded for further analysis.

Results
Synthesis of silver nanoparticles
Silver nanoparticles were successfully synthesized through the bio-reduction of silver ions using plant extracts from *C. occidentalis* and *A. pungens*. The reduction process was indicated by a distinct color change in the reaction mixture, transitioning to a dark brown hue, signifying the formation of nanoparticles (Fig. 2). This color shift is attributed to the presence of active reducing compounds in the extracellular filtrates of the plant extracts.

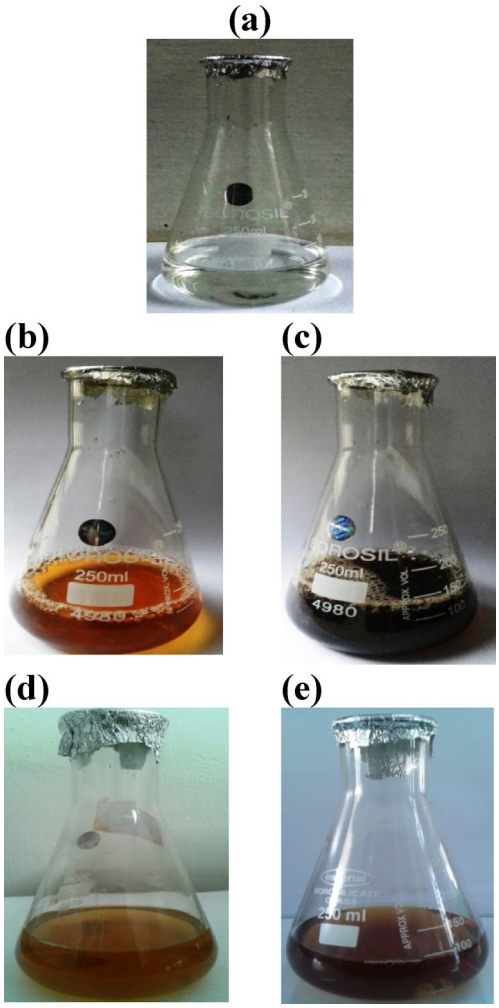

Fig. 2. Synthesis of silver nanoparticles: **(A)** Silver nitrate solution; **(B)** Silver nitrate mixed with *C. occidentalis* extract; **(C)** Silver nanoparticles biosynthesized from *C. occidentalis*; **(D)** Silver nitrate mixed with *A. pungens* extract; **(E)** Silver nanoparticles biosynthesized from *A. pungens*.

Phytochemical analysis of *C. occidentalis* revealed the presence of bioactive constituents such as achrosine, emodin, anthraquinones, anthrones, apigenin, sitosterols, tannins, and xanthones, which likely contributed to the reduction process. Similarly, *A. pungens* was found to contain a range of terpenoids and aromatic compounds, including azulene, borneol, camphene, eudesmol, geraniol, limonene, linalool, pinene, terpineol, and thujone, which played a significant role in nanoparticle synthesis.

Characterization of synthesized silver nanoparticles

UV-Visible spectroscopic analysis

The synthesis of silver nanoparticles was monitored using UV-Visible absorption spectroscopy. Aliquots (0.2 mL) were collected from the reaction mixture at regular intervals, diluted with 2 mL of deionized water, and analyzed using a UV-1601 PC Shimadzu spectrophotometer at room temperature. The progression of Ag^{+} bioreduction was evident from the gradual color change of the reaction mixture, shifting to a brownish-yellow hue after 24 h of incubation. This color intensification correlated with increased incubation time, likely due to the excitation of Surface Plasmon Resonance (SPR) and the reduction of $AgNO_3$. In contrast, the control sample containing only $AgNO_3$ (without plant extract) exhibited no color change, indicating no nanoparticle formation. The UV-Vis spectra confirmed the synthesis of silver nanoparticles, with characteristic SPR absorption peaks observed at 420 nm for *C. occidentalis* (Fig. 3a) and 425 nm for *A. pungens* (Fig. 3b). These distinct peaks serve as confirmation of nanoparticle formation and stability over time.

SEM analysis with EDX studies

SEM analysis (JEOL-MODEL 6390) revealed the formation of high-density, irregularly distributed silver nanoparticles synthesized using *C. occidentalis* (Fig. 4a & b) and *A. pungens* (Fig. 4c & d) extracts, with sizes ranging from 60 to 180 nm. The silver nanoparticles exhibited spherical and cylindrical morphologies, aggregating due to hydrogen bonding and electrostatic interactions with bio-organic capping agents. Aggregated

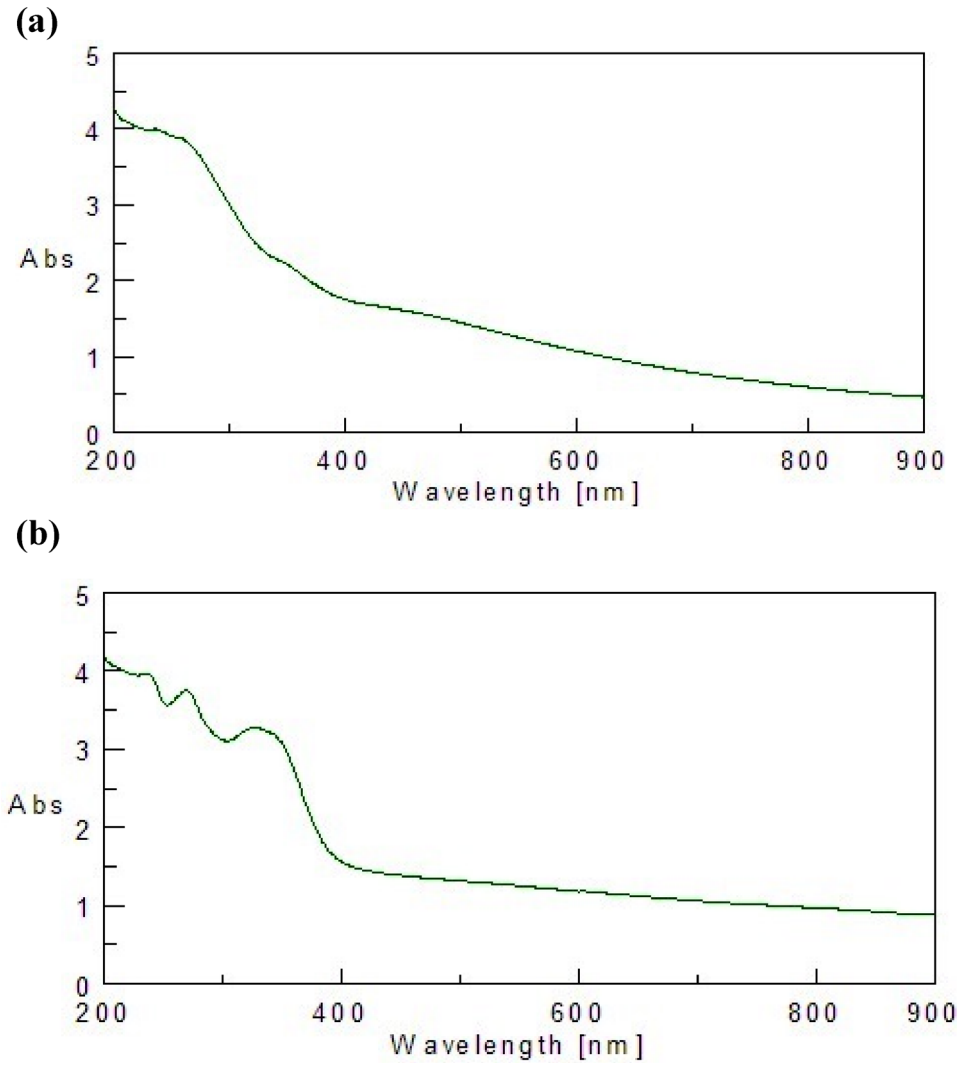

Fig. 3. UV–Visible spectra of silver nanoparticles synthesized using aqueous leaf extracts of *C. occidentalis***(a)** and *A. pungens***(b)**.

forms with sizes between 25 and 30 nm were also observed, consistent with particle accumulation patterns during solvent evaporation on flat surfaces. EDX analysis confirmed strong silver signals alongside peaks for Cl, C, and O atoms. The EDX spectra showed silver peaks around 3 kV. Quantitative data indicated that *C. occidentalis* nanoparticles contained 71.87% Ag, 10.29% C, and 17.84% O (Fig. 5a), while *A. pungens* samples showed 75.30% Ag, 9.26% C, 15.44% O, and 5.30% Cl (Fig. 5b).

Fourier transform infrared spectroscopic analysis

Significant FTIR peaks were recorded for the *C. occidentalis* leaf extract (Fig. 6a) at 3403.06, 2145.50, 1700.50, 1649.92, 1424.35, 1365.84, 1231.94, 1093.44, 1020.82, 656.63, 598.61, 547.46, 488.41, and 445.14 cm^{-1}. In contrast, *A. pungens* (Fig. 6b) exhibited peaks at 3438.20, 3007.83, 2829.80, 2146.79, 1704.41, 1652.49, 1424.85, 1363.65, 1227.84, 1093.57, 1027.74, 903.40, 751.81, 651.36, 595.02, 544.08, 476.21, and 446.42 cm^{-1}. These spectral bands indicate the presence of biomolecules involved in the capping and stabilization of silver nanoparticles, as demonstrated in the IR spectra of both plant extracts. The FTIR spectra of the synthesized silver nanoparticles revealed the existence of various functional groups, including alkanes, methylene groups, alkenes, amines, and carboxylic acids.

X-ray diffraction analysis

The XRD patterns confirm the crystalline structure of silver nanoparticles synthesized via the green method. In addition to the characteristic peaks associated with silver nanoparticles, the patterns display extra, unassigned peaks. These may correspond to crystalline bio-organic compounds derived from the plant extracts of *C. occidentalis* (Fig. 7a) and *A. pungens* (Fig. 7b). The XRD results further support the findings from UV–Vis spectroscopy, providing strong evidence for the formation of silver nanocrystals.

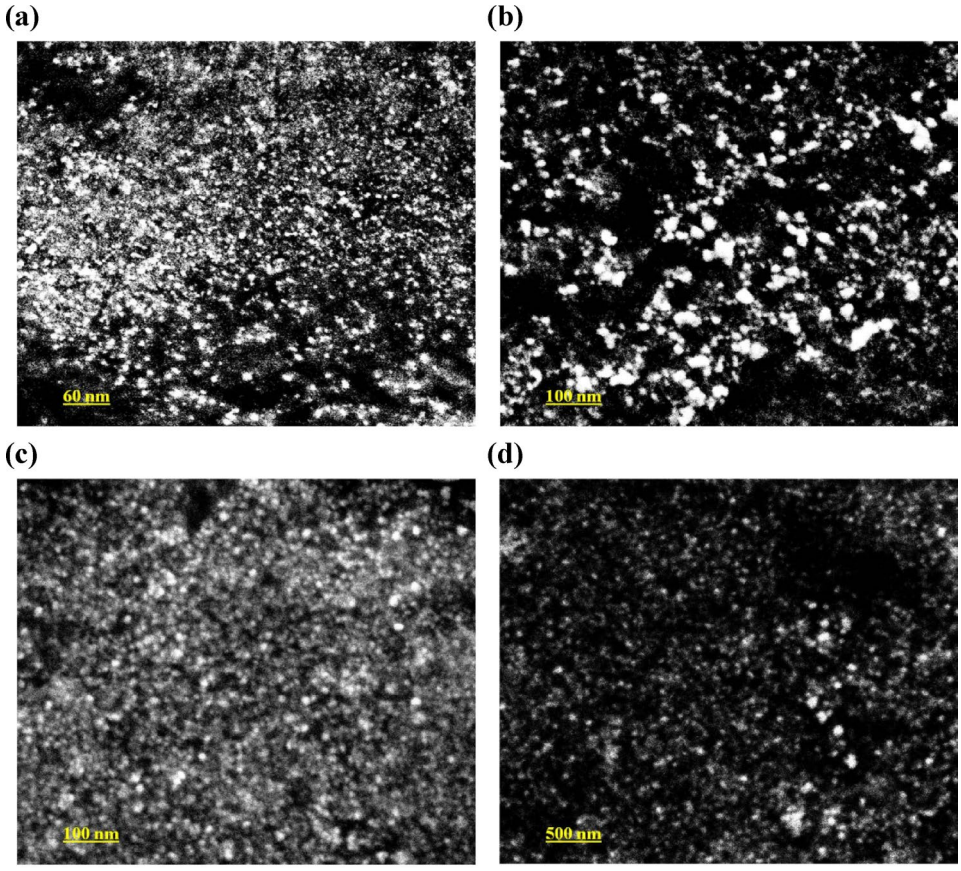

Fig. 4. SEM images displaying the morphology of silver nanoparticles synthesized using *C. occidentalis***(a & b)** and *A. pungens* leaf extracts **(c & d)**.

Zeta potential and dynamic light scattering analysis

To evaluate the colloidal stability of oxide nanoparticles, silver nanoparticles with an approximate size of 100 nm were analyzed in both distilled water and cell culture media. In distilled water, zeta potential measurements revealed that the synthesized silver nanoparticles exhibited a surface charge of +5 mV, indicating moderate colloidal stability (Fig. 8a). When introduced into biological environments, such as systems containing parasitic nematodes, the positively charged nanoparticles showed strong interactions with negatively charged parasitic particles, likely due to enhanced protein adsorption on the nanoparticle surfaces. The particle size distribution of the synthesized silver nanoparticles was assessed using dynamic light scattering. The analysis confirmed an average particle diameter of approximately 100 nm, consistent with the expected nanoparticle size. These findings are illustrated in Fig. 8b, highlighting the particle characteristics in *C. occidentalis* extracts.

Infectivity and nematicidal activity against M. incognita treated with AgNPs

The nematicidal efficacy of silver nanoparticles (AgNPs), synthesized using *C. occidentalis* and *A. pungens*, was evaluated against *M. incognita* second-stage juveniles (J2) at varying concentrations of 0.1, 0.3, 0.5, 0.7, and 1.0 mg/L. A dose-dependent increase in juvenile mortality was observed following nanoparticle exposure (Fig. 9a & b). At the lower concentrations of 0.1 mg/L and 0.3 mg/L, mortality rates ranged from 10 to 30%. With an intermediate concentration of 0.5 mg/L, mortality reached 50%, while higher concentrations of 0.7 mg/L and 1.0 mg/L resulted in significantly elevated mortality rates of 70–90%. The lethal concentration required to kill 50% of the nematode population (LC_{50}) was determined to be 0.5 mg/L in this study (Fig. 9a & b). Field trials were conducted on tomato plants to evaluate the impact of AgNPs treated nematodes. Nematodes exposed to silver nanoparticles were inoculated into the roots of tomato plants. After a period of 10 days, the roots were harvested, stained, and subsequently de-stained using phenol crystals for microscopic examination under a stereo microscope. The results revealed that in control plants, a higher number of juvenile nematodes were present within the root tissues. In contrast, at lower concentrations of AgNPs, juveniles were predominantly observed on the root surface with limited penetration (Fig. 10c & d). Notably, at higher AgNPs concentrations, juvenile nematodes were entirely absent from the roots, indicating a significant inhibitory effect on root invasion (Fig. 10e & f). In the absence of treatment with biosynthesized nanoparticles, nematode infestation was evident within the root nodules, as illustrated in Fig. 10a and b.

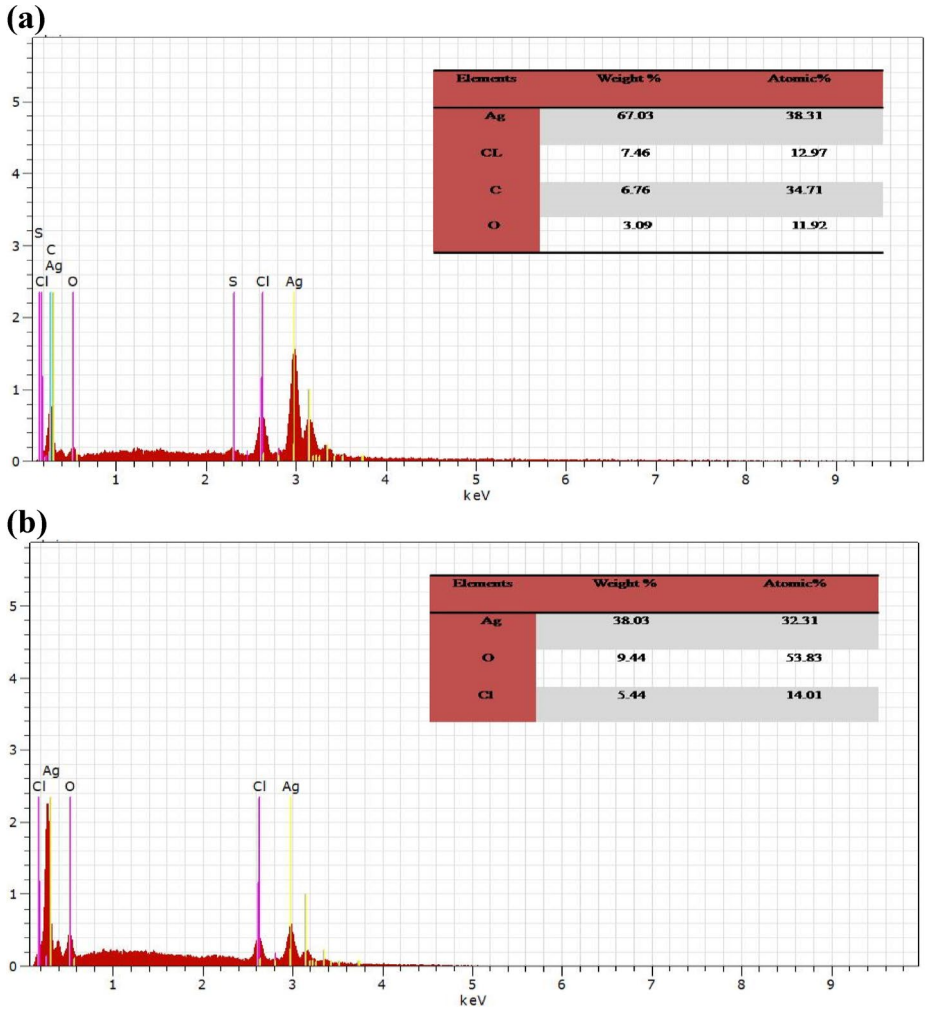

Fig. 5. EDX spectrum of silver nanoparticles synthesized using *C. occidentalis* leaf extract **(a)** and *A. pungens* leaf extract **(b)**.

Discussion

The Root-knot nematodes (*Meloidogyne* spp.) are among the most destructive plant pathogens, significantly impacting agricultural productivity in tropical, subtropical, and temperate regions[27–29]. These nematodes are regarded as the most important genus of plant-parasitic nematodes, causing yield losses of up to 16.9% annually[8,30]. Given the environmental risks associated with synthetic pesticides, there is a growing interest in plant- and microbe-based biocontrol agents. These natural alternatives exhibit biodegradability, reduced toxicity to non-target species, and a commitment to environmental sustainability[31]. Creating eco-friendly solutions has the potential to tackle pesticide resistance and encourage sustainable agricultural practices[32–35]. Previous studies have emphasized the larvicidal capabilities of plant extracts, and it has been noted that silver nanoparticles can interfere with the growth and reproduction of nematodes[36,37].

AgNPs nanoparticles exhibit considerable promise across various fields of study, with biologically synthesized variants becoming increasingly important due to technological advancements and enhanced scientific methods. Among biological approaches, plant-mediated synthesis stands out for its efficiency and simplicity, offering distinct advantages compared to microbial methods, which tend to be labor-intensive and challenging to maintain over extended periods[38–41]. A variety of plant species have been successfully utilized for the synthesis of silver nanoparticles, including *Azadirachta indica*[42,43], *Aloe vera*[44,45], *Plumeria obtusa*[46], *Plumeria pudica*[47], *Nelumbo nucifera*[48], *Emblica officinalis*[49,50] and *Medicago sativa* sprouts[51,52]. Photosynthesized silver nanoparticles are currently being investigated as nematicidal agents, emphasizing their environmentally friendly characteristics, minimal effects on non-target organisms, and distinct mechanisms of action in contrast to conventional chemical pesticides[53–55].

The bio-reduction of silver ions in the extracellular filtrate resulted in a distinct dark brown coloration, signifying the formation of nanoparticles. The observed color change correlates with the excitation of surface plasmon resonance (SPR), which arises from the collective oscillation of conduction electrons. The SPR effect is characterized by a rise in absorbance that corresponds with the concentration of reducing agents as time progresses[56,57]. A clear SPR absorption band was observed in the range of 400 to 420 nm after 24 h, validating

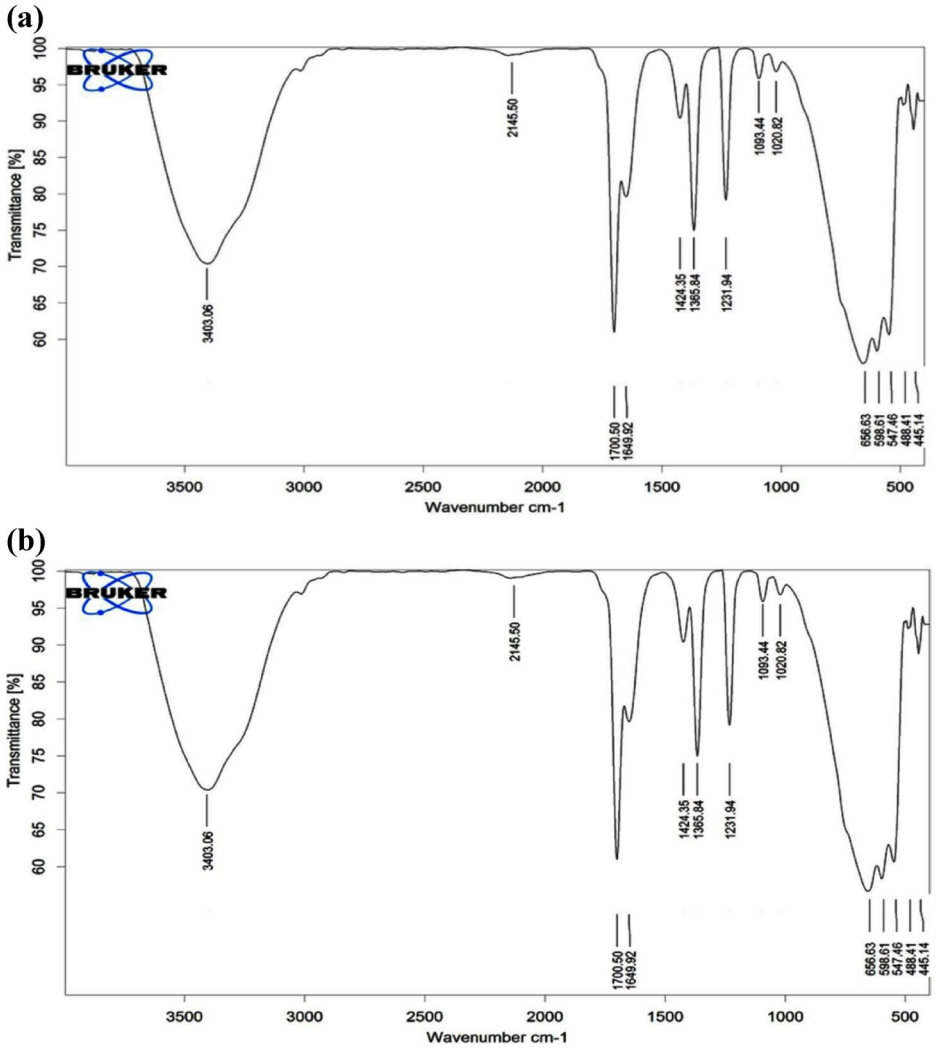

Fig. 6. FTIR spectra of vacuum-dried AgNPs synthesized from *C. occidentalis***(a)** and *A. pungens* leaf extracts **(b)**.

the synthesis of silver nanoparticles (AgNPs)[58,59]. Comparable results were observed for *C. occidentalis* and *A. pungens* extracts, where a dark color emerged after the addition of $AgNO_3$, reinforcing the reduction of silver ions and the excitation of surface plasmon resonance in the formation of AgNPs.

The SEM analysis, conducted with a 10 kV Ultra High-Resolution Scanning Electron Microscope (FEI QUANTA-200 SEM), demonstrated that silver nanoparticles synthesized using 10% *C. occidentalis* and *A. pungens* leaf broth at 65 °C were predominantly spherical, exhibiting sizes ranging from 35 to 100 nm. The stability of these nanoparticles in solution for up to 8 weeks indicates that the plant extracts provided effective capping. Comparable studies have reported silver nanoparticles ranging from 55 to 80 nm, with both spherical and triangular morphologies synthesized using sundried biomass from *C. camphora* leaves[60]. Furthermore, *A. indica*-mediated synthesis produced polydisperse silver nanoparticles displaying both spherical and plate-like structures within the 5–35 nm range[61]. The current findings also observed occasional cubical nanoparticles with uniform shapes. Given that nanoparticle morphology significantly influences their optical and electronic properties, as established by Xu and Kall[62] the observed variations in shape may impact their functional characteristics.

The EDX analysis, coupled with SEM, provided detailed elemental composition, confirming the presence of silver nanoparticles through a strong silver signal and high atomic percentage[63]. This aligns with findings from *T. viride*-mediated silver nanoparticle synthesis[64–66]. A characteristic optical absorption peak near 3 keV, typical of metallic silver due to surface plasmon resonance, was observed[67,68]. A minor oxygen signal likely originated from organic residues, such as enzymes or proteins from the leaf extract. This supports reports indicating that plant-mediated nanoparticles are stabilized by capping organic materials from the extract. Comparable spherical silver nanoparticles (< 100 nm) were previously synthesized using Morinda leaf extract[69,70].

FTIR analysis of *C. occidentalis* and *A. pungens* extracts indicated the presence of significant functional groups related to flavonoids, triterpenoids, and polyphenols, implying their involvement in the synthesis and stabilization of silver nanoparticles[71,72]. Terpenoids showed the ability to oxidize aldehyde groups into carboxylic

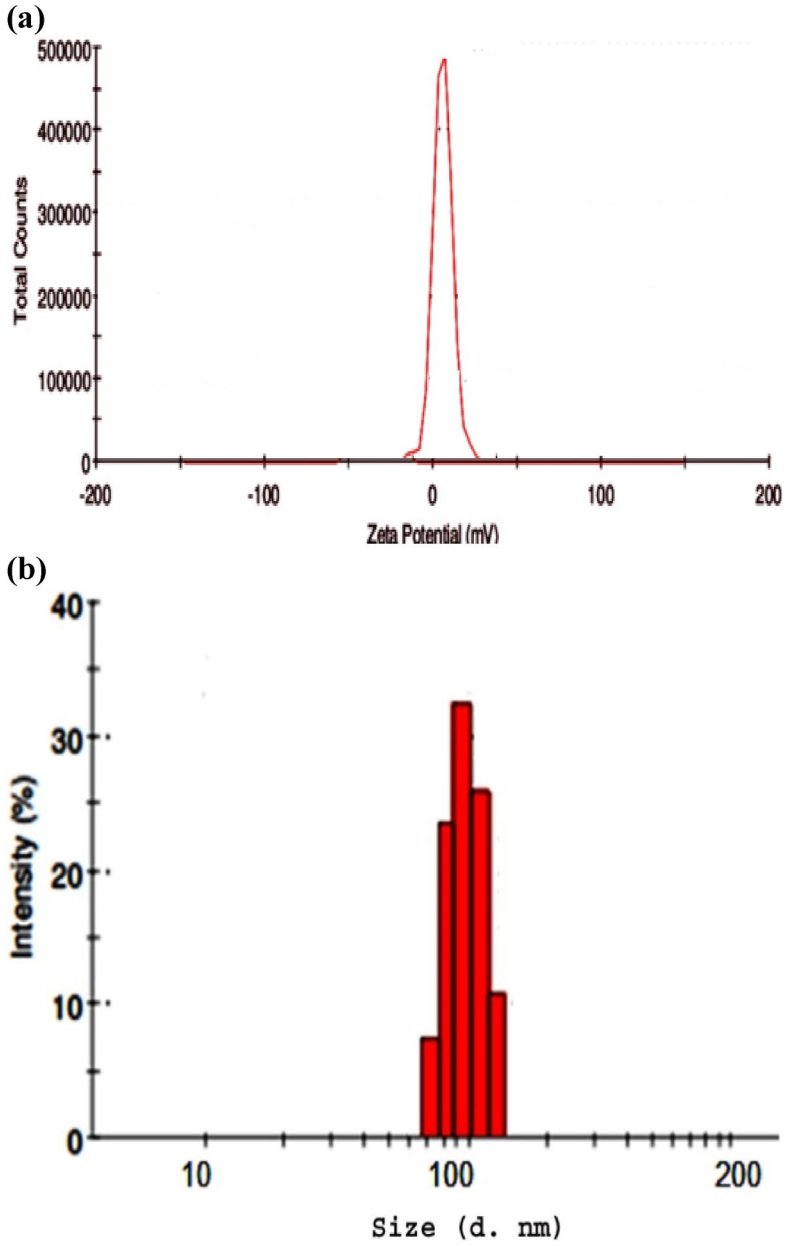

Fig. 7. XRD patterns of silver nanoparticles synthesized with *C. occidentalis***(a)** and *A. pungens* leaf extracts **(b)**.

acids in the presence of metal ions, while amide groups contributed to the enzymatic activity that facilitated the reduction and stabilization of nanoparticles[73,74]. Additionally, polyphenols played a vital role as effective reducing agents in the production of nanoparticles[75,76]. DLS and zeta potential analyses confirmed the size and surface charge of the nanoparticles, demonstrating a stable colloidal dispersion without aggregation[77,78].

The XRD analysis revealed clear diffraction peaks at 32.20°, 27.64°, and 25.30°, corresponding to the (39), (79), and (100) planes of face-centred cubic (fcc) silver. These results are consistent with earlier research that indicates AgNPs produced using *Azadirachta indica* leaf extract demonstrated comparable crystallinity and antibacterial properties[79,80]. The face-centered cubic structure of silver nanoparticles was further validated by XRD patterns documented by Shameli et al.[81] and Khalil et al.[82]. Moreover, the AgNPs produced with the broths of *Cassia fistula* flowers and *Moringa oleifera* leaves exhibited crystalline properties that align with previous studies[83,84]. In contrast, pure silver ions typically show peaks at 2θ values of 7.9°, 11.4°, 17.8°, 30.38°, and 44°[85]. The observed XRD patterns suggest that the bioorganic components may play a role in facilitating crystallization on the surface of the nanoparticles.

Green-synthesized AgNPs demonstrate significant nematicidal activity against *Pratylenchus brachyurus*, highlighting their potential as eco-friendly alternatives to conventional chemical nematicides. Their application may reduce environmental contamination commonly associated with synthetic treatments[86]. This study reveals that silver nanoparticles synthesized through green methods using *C. occidentalis* and *A. pungens* exhibit

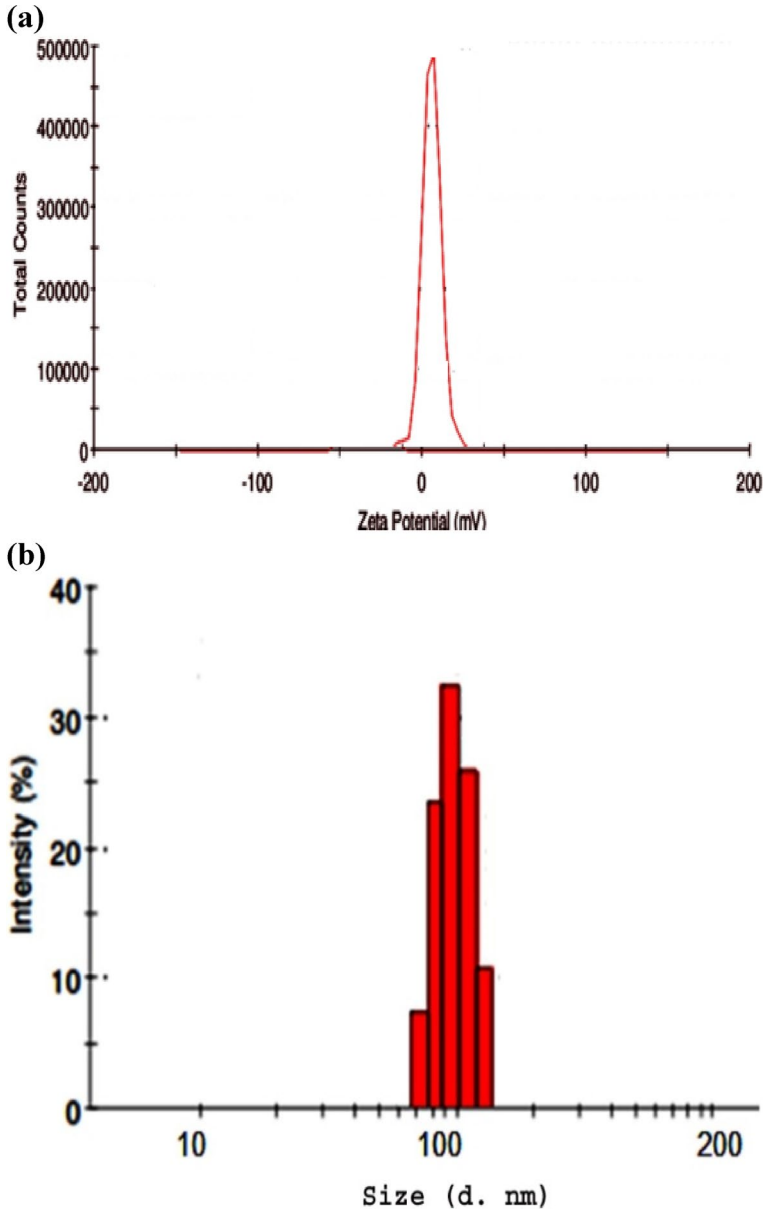

Fig. 8. Zeta potential **(a)** and DLS analysis **(b)** of AgNPs synthesized using *C. occidentalis*.

notable nematicidal activity against *M. incognita*. The AgNPs caused a concentration-dependent mortality in J2 juveniles, with observed mortality rates of 10% at 100 ppm and 30% at 300 ppm. Increased levels resulted in heightened lethality, demonstrating 50% mortality at 500 ppm, escalating to 70% and 90% at 700 ppm and 900 ppm, respectively. The results underscore the strong nematicidal capabilities of AgNPs, consistent with earlier research on their wide-ranging biological effects. The toxicity of AgNPs arises from their interactions with cellular components, as they bind to sulfur-containing proteins and phosphorus-rich compounds such as DNA, resulting in the denaturation of essential enzymes and organelles[87,88]. This mechanism of action is supported by studies showing comparable interactions of nanoparticles with proteins and carbohydrates on the surfaces of silver and gold nanoparticles[89–91]. Furthermore, exposure to AgNPs in the environment presents ecological concerns, as it has the potential to interfere with the reproductive processes of organisms such as *Caenorhabditis elegans*, which could lead to a decline in population densities[92–94].

This study identifies silver nanoparticles (AgNPs) as the most effective treatment, achieving the highest juvenile mortality in both lab and field settings. Their eco-friendly profile and low toxicity to non-target organisms support their use as sustainable bio-pesticides. AgNPs also significantly reduced nematode egg and cell development with minimal phenotypic changes. Further research is needed to assess their long-term effects on nematode physiology and soil interactions. Although standardized extraction minimized variability, natural fluctuations remain a challenge. AgNPs showed good short-term stability, but encapsulation may enhance field shelf-life. Overall, the one-pot green synthesis using *Cassia occidentalis* and *Alternanthera pungens* presents a scalable, cost-effective alternative to chemical nematicides, pending pilot-scale and economic validation.

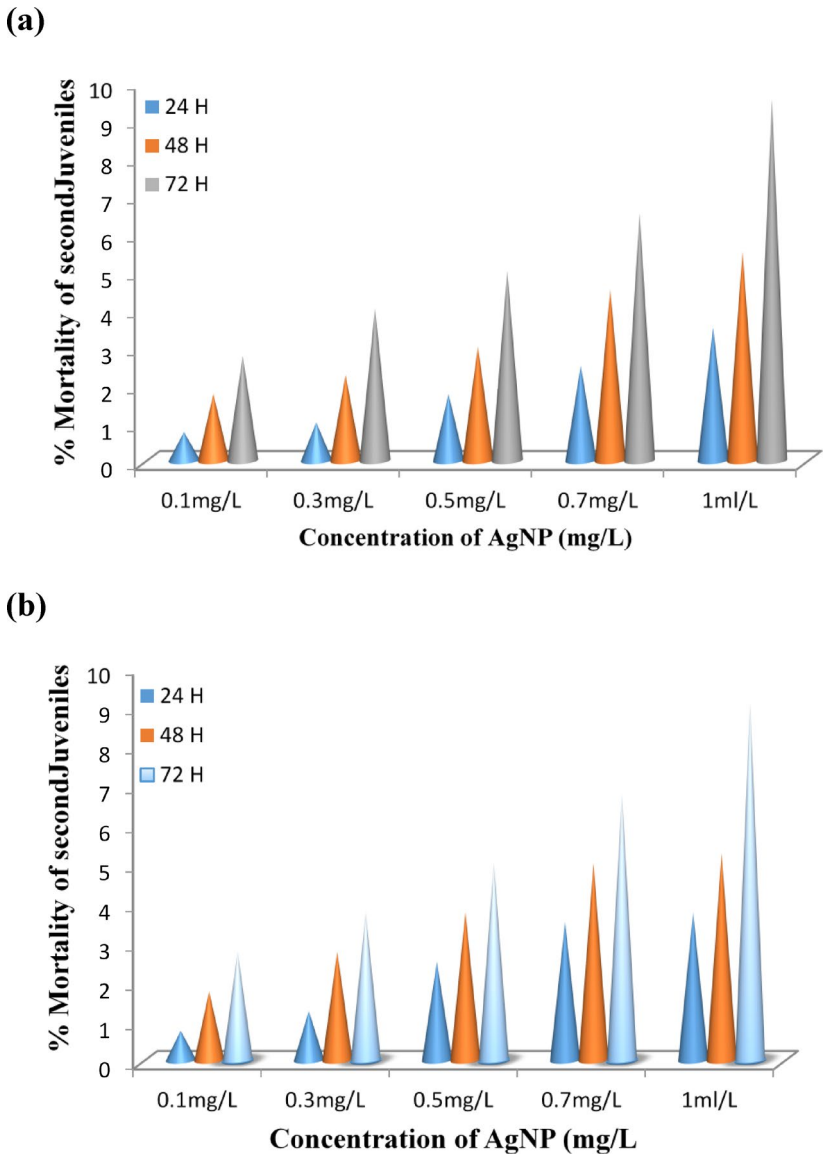

Fig. 9. LC_{50} of AgNPs derived from *C. occidentalis*(**a**) and *A. pungens*(**b**) against *M. incognita* J2.

Conclusion

The current study demonstrates that AgNPs can be successfully synthesized environmentally using leaf extracts from *C. occidentalis* and *A. pungens*. The nanoparticles possess distinct diameters of approximately 100 nm. The effectiveness of the plant extracts as capping and reducing agents was validated by thorough characterization. Higher concentrations led to a significant decrease in nematode populations, illustrating the intense nematicidal activity of the synthesized AgNPs against *M. incognita*. The LC_{50} values indicated effective nematode mortality even at moderate concentrations. The infectivity tests on tomato plants further confirmed the potential of AgNPs in reducing nematode infectivity. Overall, the study highlights that *C. occidentalis* and *A. pungens* extracts facilitate the eco-friendly synthesis of AgNPs and confer broad-spectrum biological activities, including antioxidant, antiviral, cytotoxic, and nematicidal effects. These findings suggest that AgNPs synthesized via green methods could be sustainable and effective alternatives to conventional synthetic pesticides for managing *M. incognita* infestations.

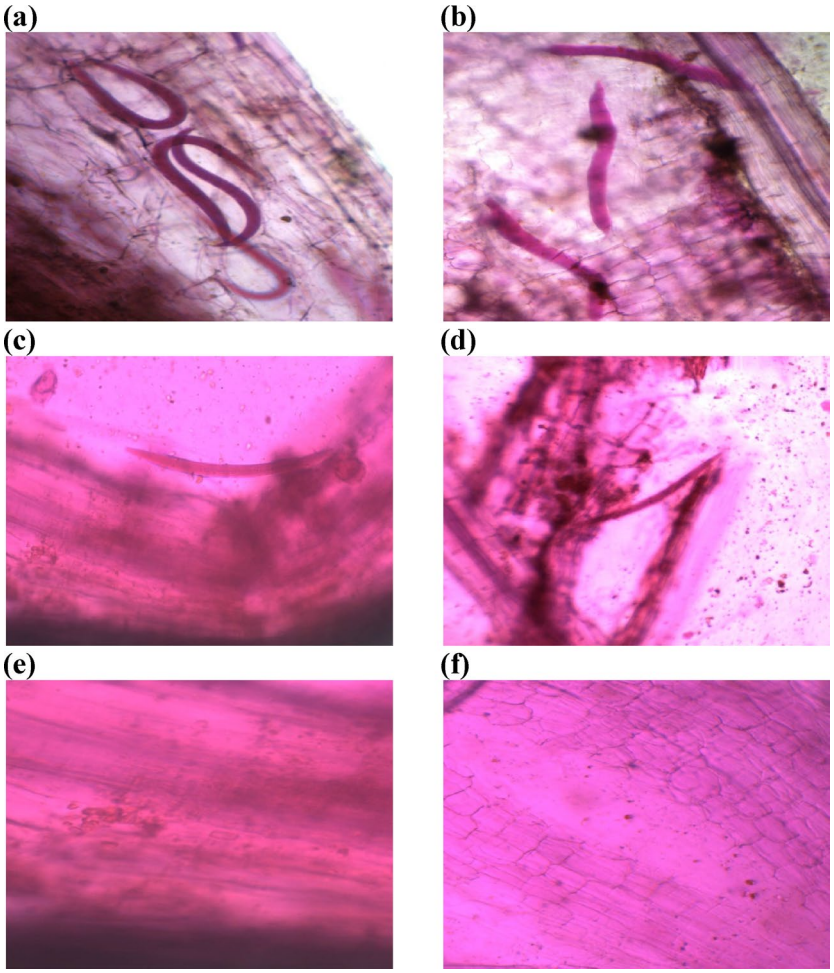

Fig. 10. Nematicidal effects of AgNPs derived from *C. occidentalis* on *M. incognita* in control **(a)** and treated samples at 0.1 mg/L **(c)** and 0.7 mg/L **(e)**. Similarly, AgNPs from *A. pungens* were tested in control **(b)** and at 0.1 mg/L **(d)** and 0.7 mg/L **(f)** concentrations.

Data availability

The data supporting the findings of this study are available within the article. Additional raw datasets generated during the study are available from the corresponding author upon reasonable request.

Received: 28 March 2025; Accepted: 15 July 2025
Published online: 19 July 2025

References

1. El-Saadony, M. T. et al. Control of foliar phytoparasitic nematodes through sustainable natural materials: current progress and challenges. *Saudi J. Biol. Sci.* **28**, 7314–7326 (2021).
2. Soomro, M. H., Iqbal, E. & Kazi, F. *Textbook of Plant Nematology* (National Nematological Research Center, University of Karachi, 2022). https://doi.org/10.33804/978.969.23704.0.0
3. Quillen, A. C., Peshkov, A., Wright, E. & McGaffigan, S. Metachronal waves in concentrations of swimming *Turbatrix aceti* nematodes and an oscillator chain model for their coordinated motions. *Phys. Rev. E***104**, 014412 (2021).
4. Singh, A. K. et al. Nematode genome announcement: A draft genome of seed gall nematode, Anguina tritici. *Journal Nematology* **55**, 20230031 (2023).
5. Skantar, A. M. Anguina tritici (wheat seed gall nematode). *CABI Compendium* Preprint at (2018). https://doi.org/10.1079/cabicompendium.5388
6. Berkeley, M. J. Vibrio forming cysts on the roots of cucumbers. *Gardener's Chron. Agric. Gazette*. **14**, (1855).
7. Sumita, K. & Vivekananda, Y. A Southern root-knot nematode (*Meloidogyne incognita*) first reported on cucumber in Manipur. *Indian J. Agric. Res.*https://doi.org/10.18805/IJARe.A-6105 (2023).
8. Dutta, T. K., Khan, M. R. & Phani, V. Plant-parasitic nematode management via biofumigation using brassica and non-brassica plants: current status and future prospects. *Curr. Plant. Biology*. **17**, 17–32 (2019).
9. Yadav, S. P. et al. Management of phyto-parasitic nematodes using bacteria and fungi and their consortia as biocontrol agents. *Environmental Science: Advances*https://doi.org/10.1039/D4VA00216D (2025).
10. Barber, C. A. *A Tea-Eelworm Disease in South India. Madras (India: Presidency). Department of Land Records and Agriculture. Agricultural Branch* vol. 2 (1901).

11. Suman, T. Y., Elumalai, D., Kaleena, P. K. & Rajasree, S. R. R. GC–MS analysis of bioactive components and synthesis of silver nanoparticle using *Ammannia baccifera* aerial extract and its larvicidal activity against malaria and filariasis vectors. *Ind. Crops Prod.***47**, 239–245 (2013).
12. Rani Rajpal, V. et al. Exploring metal and metal-oxide nanoparticles for nanosensing and biotic stress management in plant systems. *Curr. Res. Biotechnol.* **7**, 100219 (2024).
13. Zhou, X. et al. Nanoparticles: a promising tool against environmental stress in plants. *Frontiers Plant. Science* **15**, 1509047 (2025).
14. Antunes Filho, S. et al. Biosynthesis of nanoparticles using plant extracts and essential oils. *Molecules* **28**, 3060 (2023).
15. Marcon, L., Oliveras, J. & Puntes, V. F. In situ nanoremediation of soils and groundwaters from the nanoparticle's standpoint: A review. *Sci. Total Environ.***791**, 148324 (2021).
16. Pasha, A. et al. Role of biosynthesized Ag-NPs using Aspergillus Niger (MK503444.1) in antimicrobial, Anti-Cancer and Anti-Angiogenic activities. *Front. Pharmacol.* **12**, 812474 (2021).
17. Kulkarni, D. et al. Biofabrication of nanoparticles: sources, synthesis, and biomedical applications. *Frontiers Bioeng. Biotechnology* **11**, 1159193 (2023).
18. Sampath, G. et al. Biologically synthesized silver nanoparticles and their diverse applications. *Nanomaterials***12**, 3126 (2022).
19. Anees Ahmad, S. et al. Bactericidal activity of silver nanoparticles: A mechanistic review. *Mater. Sci. Energy Technol.* **3**, 756–769 (2020).
20. Rodrigues, A. S. et al. Advances in silver nanoparticles: A comprehensive review on their potential as antimicrobial agents and their mechanisms of action elucidated by proteomics. *Front. Microbiol.***15**, 1440065 (2024).
21. Velayutham, K. et al. Larvicidal activity of green synthesized silver nanoparticles using bark aqueous extract of *Ficus racemosa* against *Culex quinquefasciatus* and *Culex gelidus*. *Asian Pac. J. Trop. Med.***6**, 95–101 (2013).
22. Oladeji, O. S., Adelowo, F. E. & Oluyori, A. P. The genus Senna (Fabaceae): A review on its traditional uses, botany, phytochemistry, Pharmacology and toxicology. *South. Afr. J. Bot.* **138**, 1–32 (2021).
23. Silva, M. G. B. et al. Acute and subacute toxicity of *Cassia occidentalis* L. stem and leaf in Wistar rats. *J. Ethnopharmacol.***136**, 341–346 (2011).
24. Yadav, J. P. et al. *Cassia occidentalis* L.: A review on its ethnobotany, phytochemical and pharmacological profile. *Fitoterapia***81**, 223–230 (2010).
25. Rainatou, B. et al. Phytochemical Study and In Vitro Biological Activities of Hibiscus panduriformis Burm. f. (Malvaceae), Alternanthera pungens Kunth (Amaranthaceae), and Wissadula rostrata (Schumach.) Hook. f. (Malvaceae). *BioMed research international* 8289750 (2023). (2023).
26. Singla, R. K. et al. The genus alternanthera: phytochemical and ethnopharmacological perspectives. *Frontiers Pharmacology* **13**, 769111 (2022).
27. Sharma, M., Devi, S. & Chand, S. Biocontrol strategies for sustainable management of root-knot nematodes. *Physiol. Mol. Plant Pathol.***136**, 102548 (2025).
28. Mukhtar, T., Hussain, M. A., Kayani, M. Z. & Aslam, M. N. Evaluation of resistance to root-knot nematode (Meloidogyne incognita) in Okra cultivars. *Crop Prot.* **56**, 25–30 (2014).
29. Kayani, M. Z., Mukhtar, T. & Hussain, M. A. Ul-Haque, M. I. Infestation assessment of root-knot nematodes (Meloidogyne spp.) associated with cucumber in the Pothowar region of Pakistan. *Crop Prot.* **47**, 49–54 (2013).
30. Pulavarty, A., Egan, A., Karpinska, A., Horgan, K. & Kakouli-Duarte, T. Plant parasitic nematodes: A review on their behaviour, host interaction, management approaches and their occurrence in two sites in the Republic of Ireland. *Plants*https://doi.org/10.3390/plants10112352 (2021).
31. Sati, A., Ranade, T. N., Mali, S. N., Yasin, A., Pratap, A. & H. K. & Silver nanoparticles (AgNPs): comprehensive insights into bio/synthesis, key influencing factors, multifaceted applications, and toxicitya 2024 update. *ACS Omega*. **10**, 7549–7582 (2025).
32. Khursheed, A. et al. Plant based natural products as potential ecofriendly and safer biopesticides: A comprehensive overview of their advantages over conventional pesticides, limitations and regulatory aspects. *Microb. Pathog.***173**, 105854 (2022).
33. Souto, A. L. et al. Plant-derived pesticides as an alternative to pest management and sustainable agricultural production: Prospects, applications and challenges. *Molecules***26**, 4835 (2021).
34. Barathi, S., Sabapathi, N., Kandasamy, S. & Lee, J. Present status of insecticide impacts and eco-friendly approaches for remediation-A review. *Environ. Res.***240**, 117432 (2024).
35. Ngegba, P. M., Cui, G., Khalid, M. Z. & Zhong, G. Use of botanical pesticides in agriculture as an alternative to synthetic pesticides. *Agriculture* **12**, 600 (2022).
36. Amarasinghe, L. D., Wickramarachchi, P. A. S. R., Aberathna, A. A. A. U., Sithara, W. S. & De Silva, C. R. Comparative study on larvicidal activity of green synthesized silver nanoparticles and *Annona glabra* (Annonaceae) aqueous extract to control *Aedes aegypti* and *Aedes albopictus* (Diptera: Culicidae). *Heliyon***6**, e04322 (2020).
37. Xu, L. et al. Silver nanoparticles: Synthesis, medical applications and biosafety. *Theranostics***10**, 8996–9031 (2020).
38. Rezghi Rami, M. & Meskini, M. Ebadi sharafabad, B. Fungal-mediated nanoparticles for industrial applications: synthesis and mechanism of action. *J. Infect. Public Health*. **17**, 102536 (2024).
39. Abuzeid, H. M., Julien, C. M., Zhu, L. & Hashem, A. M. Green synthesis of nanoparticles and their energy storage, environmental, and biomedical applications. *Crystals***13**, 1576 (2023).
40. Osman, A. I. et al. Synthesis of green nanoparticles for energy, biomedical, environmental, agricultural, and food applications: A review. *Environ. Chem. Lett.***22**, 841–887 (2024).
41. Upadhyay, R. & Bano, S. A. Review on terpenoid synthesized nanoparticle and it's antimicrobial activity. *Orient. J. Chem.***39**, 452–462 (2023).
42. Kumari, S. A., Patlolla, A. K. & Madhusudhanachary, P. Biosynthesis of silver nanoparticles using *Azadirachta indica* and their antioxidant and anticancer effects in cell lines. *Micromachines***13**, 1416 (2022).
43. Ahmed, S., Saifullah, Ahmad, Swami, M., Swami, B. L. & Ikram, S. Green synthesis of silver nanoparticles using *Azadirachta indica* aqueous leaf extract. *J. Radiat. Res. Appl. Sci.***9**, 1–7 (2016).
44. Arshad, H., Saleem, M., Pasha, U. & Sadaf, S. Synthesis of *Aloe vera*-conjugated silver nanoparticles for use against multidrug-resistant microorganisms. *Electron. J. Biotechnol.***55**, 55–64 (2022).
45. Tippayawat, P., Phromviyo, N., Boueroy, P. & Chompoosor, A. Green synthesis of silver nanoparticles in *aloe vera* plant extract prepared by a hydrothermal method and their synergistic antibacterial activity. *PeerJ***4**, e2589 (2016).
46. Khanam, B. R. et al. Green synthesis of silver nanoparticles using *Plumeria obtusa* leaves extract and concentration dependent physio-optic properties. *Mater. Today Proc.***92**, 1568–1574 (2023).
47. Suriyakala, G. et al. *Plumeria pudica* Jacq. flower extract - mediated silver nanoparticles: Characterization and evaluation of biomedical applications. *Inorg. Chem. Commun.***126**, 108470 (2021).
48. Santhoshkumar, T. et al. Synthesis of silver nanoparticles using *Nelumbo nucifera* leaf extract and its larvicidal activity against malaria and filariasis vectors. *Parasitol. Res.***108**, 693–702 (2011).
49. Ramesh, P. S., Kokila, T. & Geetha, D. Plant mediated green synthesis and antibacterial activity of silver nanoparticles using emblica officinalis fruit extract. *Spectrochim. Acta Part A Mol. Biomol. Spectrosc.* **142**, 339–343 (2015).
50. Dhar, S. A. et al. Plant-mediated green synthesis and characterization of silver nanoparticles using Phyllanthus emblica fruit extract. *Mater. Today: Proc.* **42**, 1867–1871 (2021).
51. Song, K. et al. Green nanopriming: Responses of alfalfa (*Medicago sativa* L.) seedlings to alfalfa extracts capped and light-induced silver nanoparticles. *BMC Plant Biol.***22**, 323 (2022).

52. Kokina, I., Plaksenkova, I., Jankovskis, L., Jermaļonoka, M. & Galek, R. New insights on biosynthesis of nanoparticles using plants emphasizing the use of alfalfa (Medicago sativa L). *J. Nanatechnol.* **2024**, 1–24 (2024).
53. El-Ashry, R. M. et al. Biological silicon nanoparticles maximize the efficiency of nematicides against biotic stress induced by *Meloidogyne incognita* in eggplant. *Saudi J. Biol. Sci.***29**, 920–932 (2022).
54. Nie, D. et al. Nanoparticles: A Potential and Effective Method to Control Insect-Borne Diseases. *Bioinorganic chemistry and applications* 5898160 (2023). (2023).
55. Mariyam, S. et al. Nanotechnology, a frontier in agricultural science, a novel approach in abiotic stress management and convergence with new age medicine-A review. *Sci. Total Environ.***912**, 169097 (2024).
56. Chatterjee, N., Pal, S. & Dhar, P. Green silver nanoparticles from bacteria- antioxidant, cytotoxic and antifungal activities. *Next Nanatechnol.* **6**, 100089 (2024).
57. Akhter, N. et al. Potential biological application of silver nanoparticles synthesized from *Citrus paradisi* leaves. *Sci. Rep.***14**, 29028 (2024).
58. Dhaka, A., Chand Mali, S., Sharma, S. & Trivedi, R. A review on biological synthesis of silver nanoparticles and their potential applications. *Results Chem.* **6**, 101108 (2023).
59. Tesfaye, M., Gonfa, Y., Tadesse, G., Temesgen, T. & Periyasamy, S. Green synthesis of silver nanoparticles using *Vernonia amygdalina* plant extract and its antimicrobial activities. *Heliyon***9**, e17356 (2023).
60. Huang, J. et al. Biosynthesis of silver and gold nanoparticles by novel sundried *Cinnamomum camphora* leaf. *Nanotechnology***18**, 105104 (2007).
61. Shankar, S. S., Rai, A., Ahmad, A. & Sastry, M. Rapid synthesis of Au, Ag, and bimetallic Au core–Ag shell nanoparticles using neem (*Azadirachta indica*) leaf broth. *J. Colloid Interface Sci.***275**, 496–502 (2004).
62. Xu, H. & Käll, M. Surface-plasmon-enhanced optical forces in silver nanoaggregates. *Phys. Rev. Lett.***89**, 246802 (2002).
63. Alam, M. Analyses of biosynthesized silver nanoparticles produced from strawberry fruit pomace extracts in terms of biocompatibility, cytotoxicity, antioxidant ability, photodegradation, and in-silico studies. *J. King Saud Univ. - Sci.* **34**, 102327 (2022).
64. Tomah, A. A. et al. The potential of Trichoderma-mediated nanotechnology application in sustainable development scopes. *Nanomaterials*. **13**(17), 2475. https://doi.org/10.3390/nano13172475 (2023).
65. Fayaz, A. M. et al. Biogenic synthesis of silver nanoparticles and their synergistic effect with antibiotics: A study against gram-positive and gram-negative bacteria. *Nanomed. Nanotechnol. Biol. Med.***6**, 103–109 (2010).
66. Elgorban, A. M. et al. Antimicrobial activity and green synthesis of silver nanoparticles using *Trichoderma viride*. *Biotechnol. Biotechnol. Equip.***30**, 299–304 (2016).
67. Alzahrani, E. Colorimetric detection based on localized surface plasmon resonance optical characteristics for sensing of mercury using Green-Synthesized silver nanoparticles. *J. Anal. Methods Chem.* **2020**(1), 6026312 (2020). https://doi.org/10.1155/2020/6026312
68. Bindhu, M. R. & Umadevi, M. Surface plasmon resonance optical sensor and antibacterial activities of biosynthesized silver nanoparticles. *Spectrochim. Acta Part A Mol. Biomol. Spectrosc.* **121**, 596–604 (2014).
69. Sathishkumar, G. et al. Phyto-synthesis of silver nanoscale particles using *Morinda citrifolia* L. and its inhibitory activity against human pathogens. *Colloids Surf. B, Biointerfaces***95**, 235–240 (2012).
70. Islam, A., Mandal, C. & Habib, A. Antibacterial potential of synthesized silver nanoparticles from leaf extract of *Moringa oleifera*. *J. Adv. Biotechnol. Exp. Ther.***4**, 67 (2021).
71. Zuhrotun, A., Oktaviani, D. J. & Hasanah, A. N. Biosynthesis of gold and silver nanoparticles using phytochemical compounds. *Molecules***28**, 3240 (2023).
72. Nadaf, S. J. et al. Green synthesis of gold and silver nanoparticles: Updates on research, patents, and future prospects. *OpenNano***8**, 100076 (2022).
73. Thatyana, M. et al. Advances in phytonanotechnology: A plant-mediated green synthesis of metal nanoparticles using *Phyllanthus* plant extracts and their antimicrobial and anticancer applications. *Nanomaterials***13**, 2616 (2023).
74. Mikhailova, E. O. Green silver nanoparticles: an antibacterial mechanism. *Antibiotics* **14**, 5 (2024).
75. Ying, S. et al. Green synthesis of nanoparticles: current developments and limitations. *Environ. Technol. Innov.* **26**, 102336 (2022).
76. Amini, S. M. & Akbari, A. Metal nanoparticles synthesis through natural phenolic acids. *IET Nanobiotechnol.* **13**, 771–777 (2019).
77. Bhattacharjee, S. DLS and zeta potential – What they are and what they are not? *J. Controlled Release*. **235**, 337–351 (2016).
78. Pochapski, D. J., Carvalho dos Santos, C., Leite, G. W., Pulcinelli, S. H. & Santilli, C. V. Zeta potential and colloidal stability predictions for inorganic nanoparticle dispersions: Effects of experimental conditions and electrokinetic models on the interpretation of results. *Langmuir***37**, 13379–13389 (2021).
79. Verma, A. & Mehata, M. S. Controllable synthesis of silver nanoparticles using neem leaves and their antimicrobial activity. *J. Radiat. Res. Appl. Sci.***9**, 109–115 (2016).
80. Alqahtani, O. et al. In vitro antibacterial activity of green synthesized silver nanoparticles using *Azadirachta indica* aqueous leaf extract against MDR pathogens. *Molecules***27**, 7244 (2022).
81. Shameli, K. et al. Green biosynthesis of silver nanoparticles using *Callicarpa maingayi* stem bark extraction. *Molecules***17**, 8506–8517 (2012).
82. Khalil, M. M. H., Ismail, E. H., El-Baghdady, K. Z. & Mohamed, D. Green synthesis of silver nanoparticles using Olive leaf extract and its antibacterial activity. *Arab. J. Chem.* **7**, 1131–1139 (2014).
83. Esther Arland, S. & Kumar, J. Green and chemical syntheses of silver nanoparticles: comparative and comprehensive study on characterization, therapeutic potential, and cytotoxicity. *Eur. J. Med. Chem. Rep.* **11**, 100168 (2024).
84. Asif, M. et al. Green synthesis of silver nanoparticles (AgNPs), structural characterization, and their antibacterial potential. *Dose-Response***20**, 15593258221088708 (2022).
85. Gong, P. et al. Preparation and antibacterial activity of Fe 3 O 4 @ag nanoparticles. *Nanotechnology***18**, 285604 (2007).
86. Oliveira, L. S. et al. Eco-friendly silver nanoparticles synthesized from a soybean by-product with nematicidal efficacy against *Pratylenchus brachyurus*. *Nanomaterials***14**, 101 (2023).
87. More, P. R. et al. Silver nanoparticles: Bactericidal and mechanistic approach against drug resistant pathogens. *Microorganisms*https://doi.org/10.3390/microorganisms11020369 (2023).
88. Dakal, T. C., Kumar, A., Majumdar, R. S. & Yadav, V. Mechanistic basis of antimicrobial actions of silver nanoparticles. *Frontiers Microbiology* **7**, 1831 (2016).
89. Perera, Y. R., Hill, R. A. & Fitzkee, N. C. Protein interactions with nanoparticle surfaces: Highlighting solution NMR techniques. *Isr. J. Chem.***59**, 962–979 (2019).
90. Jebali, A. et al. Nano-carbohydrates: Synthesis and application in genetics, biotechnology, and medicine. *Adv. Colloid Interface Sci.***240**, 1–14 (2017).
91. Joshi, A. S., Singh, P. & Mijakovic, I. Interactions of gold and silver nanoparticles with bacterial biofilms: Molecular interactions behind inhibition and resistance. *Int. J. Mol. Sci.***21**, 7658 (2020).
92. Dinç, B. Comprehensive toxicity assessment of silver nanoparticlesa on bacteria, human vein endothelial cells, and Caenorhabditis Elegans. *Results Chem.* **14**, 102092 (2025).
93. Wamucho, A., Heffley, A. & Tsyusko, O. V. Epigenetic effects induced by silver nanoparticles in *Caenorhabditis elegans* after multigenerational exposure. *Sci. Total Environ.***725**, 138523 (2020).

94. Luo, X. et al. Insights into the ecotoxicity of silver nanoparticles transferred from *Escherichia coli* to *Caenorhabditis elegans*. *Sci. Rep.***6**, 36465 (2016).

Author contributions

Navaneetha Krishnan Ayyankalai: Writing – original draft, Validation, Methodology, Formal analysis, Data curation, Conceptualization. Palanisamy Sundararaj: Writing – review & editing, Writing – original draft, Supervision. Manikantan Gurumoorthy Baskar: Writing – review & editing, Writing – original draft, Visualization. Nallusamy Duraisamy: Writing – review & editing, Supervision. Sakthivel Muthu: Writing – original draft, Writing – review & editing, Supervision. Mythileeswari Lakshmikanthan: Writing – original draft, Writing – review & editing, Conceptualization. Gholamreza Abdi: Writing – original draft, Validation, Methodology, Formal analysis, Data curation, Conceptualization.

Declarations

Competing interests

The authors declare no competing interests.

Additional information

Correspondence and requests for materials should be addressed to N.D., S.M. or G.A.

Reprints and permissions information is available at www.nature.com/reprints.

Publisher's note Springer Nature remains neutral with regard to jurisdictional claims in published maps and institutional affiliations.